

CHARACTERISTICS OF DISSIMILAR WELDING OF DUPLEX STAINLESS STEEL AISI 2205 TO AUSTENITIC STAINLESS STEEL AISI 201

Santirat Nansaarnng*, Narasak Duangsrikaew, Supreeya Siripattanakunkajorn

Department of Production Technology Education, Faculty of Industrial Education and Technology, King Mongkut's University of Technology Thonburi, Bangkok, 10140, Thailand

Received 16 March 2017; Revised 5 June 2017; Accepted 8 June 2017

ABSTRACT

The objective of the present work is to research the dissimilar welding of Duplex Stainless Steel AISI 2205 to Austenitic Stainless Steel AISI 201. Gas tungsten arc welding with identical parameters and procedures was used to a square butt welding with two types as cooling rate (cooling by carbon steel, copper, and copper with water cooled), and welding of speed (1.5 mm s^{-1} , 2.5 mm s^{-1} and 3.5 mm s^{-1}). Metallographic, hardness, tensile strength was examined for all specimens. The results of this research reveal that the optimum properties of the specimen were welded with parameter as cooling by copper with water cooled and welding speed 3.5 mm s^{-1} have shortest of dendrite length ($76.44 \mu\text{m}$), lowest of the width of face welded (6.04 mm), maximum hardness and tensile strength.

KEYWORDS: *Dissimilar welded; Duplex stainless steel; GTAW process; Austenitic stainless steel; Mechanical properties*

*

Corresponding authors; e-mail: santirat.nan@kmutt.ac.th, Tel +662-470-8554-6, Fax: +662-470-8557

INTRODUCTION

Engineering materials have special properties such as good mechanical properties and corrosion resistant are Stainless steels that have been used widely in variety industries and the environment. Fabrication technique for stainless steels is welding process because they have good weldability [1, 2]. Duplex stainless steels, due to higher strength and corrosion resistant when control ferrite-austenite balance in "50/50" that good for offshore oil and gas industries, petrol-chemical industries [3]. AISI 304, Austenitic stainless steels, due to excellent properties such as superior corrosion resistance, ductility, toughness, and weldability, represent the largest general groups of stainless steels, which are produced in higher tonnages than any other groups [4]. However, the price of AISI 304 relation with nickel price is relatively high and fluctuating as compared to other austenite forming elements. Manganese is cheaper element than nickel and used for developing to new austenitic stainless steel with 7 wt.% manganese to stabilize the austenite phase instead of nickel, and same properties of 18wt.% chromium. AISI 201 sheets of steel is new stainless steels with reduced nickel addition from 8 wt.% to 3 wt.%, is

it possible to replace that fails part of AISI 304 stainless steel. Wichan Chuaiphana and Loeshpahn Srijaroenpramong [5, 6] studies the effect of parameters on microstructures, mechanical properties, and corrosion behavior. The results showed that the joints made using the high welding speed exhibited smaller weld bead size, higher tensile strength and elongation, higher hardness and higher pitting corrosion potentials than those welded with medium and low welding speeds and ER309L and ER316L fillers were the good candidates to promote the pitting corrosion resistance of weld metals and were comparable with that of AISI 201 base metal. In this work, study dissimilar welded between duplex stainless steel AISI 2205 and austenitic stainless steel AISI 201 the influence of weld backing, welding speed and welding current on the mechanical properties and microstructures was investigated.

MATERIALS AND METHODS

Materials and welding procedure

Two types of stainless steel for this study was AISI 201 austenitic stainless steel and AISI 2205 duplex stainless steel. Their chemical composition was listed in Table 1. Dimensions of stainless steel plate for welding were $150 \text{ mm} \times 100 \text{ mm} \times 2 \text{ mm}$.

The experimental welding process was welding by an automatic gas tungsten arc welding (GTAW) with a square butt joint (Fig. 2) which the welding parameters were exhibited in Table 2. Fixed parameters used in this work process and procedure include: Type and size of the non-consumable for the joints investigated in this study tungsten electrode EWTh2 (Thoriated tungsten) of

2.4 mm diameter, Nozzle size = 8 mm, shielding gas flow rate of industrially pure Argon (99.99%) = 10 L mm⁻¹ and welding backing water cooled flow = 30 L mm⁻¹, Polarity = DC electrode positive. After welding, the specimens were cooled down to room temperature in the laboratory. All the welds were examined under a stereomicroscope. The widths of weld metal on face and root sides were determined by the metallographic method.

Table 1 Chemical composition

Materials	Chemical composition (wt.%)								
	C	Mn	Si	P	S	Cr	Ni	Mo	Cu
AISI 2205	0.03	1.52	0.63	0.03	0.02	23.72	5.83	3.99	0.17
AISI 201	0.07	10.43	0.43	0.05	0.01	14.40	1.73	0.11	0.92

Table 2 Welding parameters

Weld backing	Welding speed (mm s ⁻¹)	Welding current (A)	Welding voltage (V)	Heat input (kJ mm ⁻¹)
Carbon steel	1.5	85	15 ± 1	0.850
	2.5	95	14 ± 1	0.494
	3.5	110	13 ± 1	0.345
Copper	1.5	85	15 ± 1	0.850
	2.5	95	14 ± 1	0.494
	3.5	110	13 ± 1	0.345
Carbon steel	1.5	85	15 ± 1	0.850
	2.5	95	14 ± 1	0.494
	3.5	110	13 ± 1	0.345

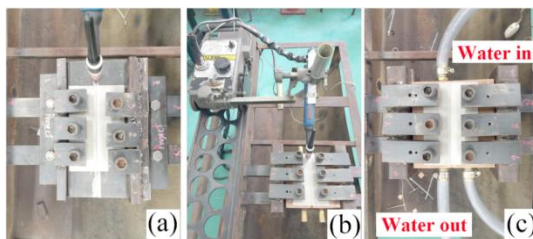


Fig. 1 Weld Backing system (a) carbon steel plate backing (b) copper plate backing (c) copper plate backing with water cooled backing.

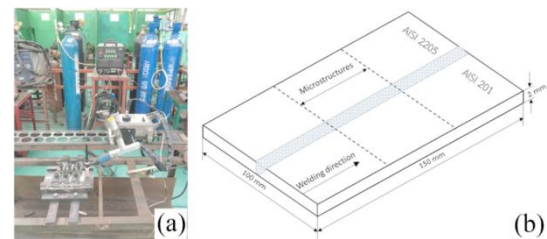


Fig. 2 Welding process (a) GTAW fixture for experimental system (b) weld sample size for metallographic and microhardness test.

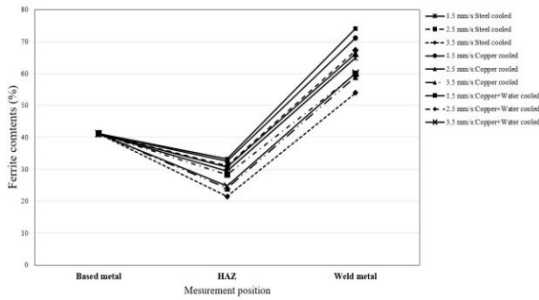


Fig. 3 The results of ferrite content measurement. Welded with welding speed at 1.5, 2.5, and 3.5 mm/s which cooled by 3 types weld backing as carbon steel (Steel cooled), copper (Copper cooled), and copper with water cooled (Copper+Water cooled).

Table 3 Microstructure of welded at AISI 2205 site

Weld backing	Welding speed (mm s ⁻¹)		
	1.5	2.5	3.5
Carbon steel			
Copper			
Copper with water cooled			

RESULTS AND DISCUSSION

The microstructure of weldment is shown in Table 3–4 present the 3 area of the weld as weld metal (WM), Heat affected zone (HAZ), and Fusion boundary (FB). Ferrite phase (light) and austenite phase (dark) was present in all area. It was found that weld metal has ferrite content more than any area because ferrite stabilizer elements from AISI 2205 and AISI 201 can be

Metallography

Microstructure examination of weldments was preparing specimens from the weld pads as shown Fig. 2 (b). welded specimens were mounted by molding epoxy, polished by SiC paper, followed by 1.0 μm Al₂O₃ powders, and then electrolytically etched in NaOH 50 g dilution in 100 ml distilled water at a voltage of 6V according to ASTM E407–07e1 [7] specification. The microstructures of different zones of interest like weld metal, HAZ and fusion boundary under different welding speed combinations were viewed and captured with an optical microscope coupled with an image analyzing software at a magnification of 100X to facilitate measuring of the details like cross-sectional areas of the face and root of weld metals

promoted ferrite stable at this area. The results of ferrite content measurement revealed that in Fig. 3 Ferrite contents in the weld metals were measured in five points of three weld area of each weld pass for all samples, with the use of Leica image analysis program. For all samples, based metal area of all weldment contains lesser amounts of delta ferrite. Fig. 3 reveals that ferrite content in the weld metal is higher than that in another area. This is related to the highest heat

input and a rapid welding speed of sample (welded with welding speed at 1.5 mm s^{-1} and weld backing with Copper with water cooled). This phenomenon indicates the effect of

cooling rate and welding speed on ultimate weld metal zone microstructure. Ferrite phase has a slow transformation to austenite under highest heat input and rapid cooling [8].

Table 4 Microstructure of welded at AISI 201 site

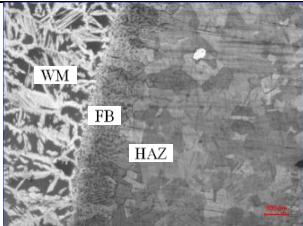
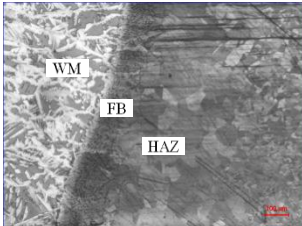
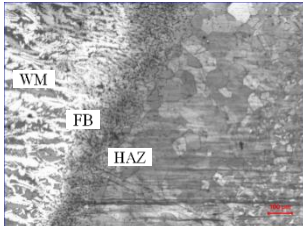
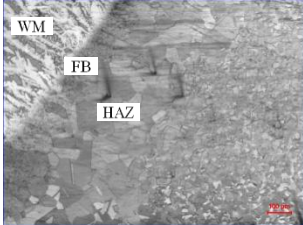
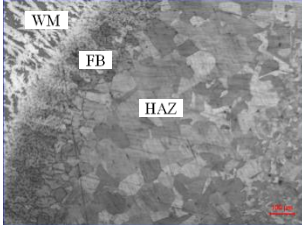
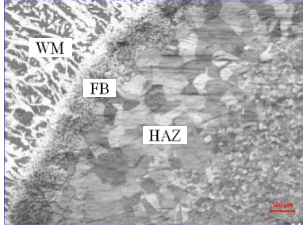
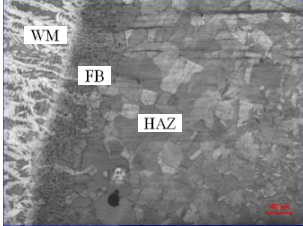
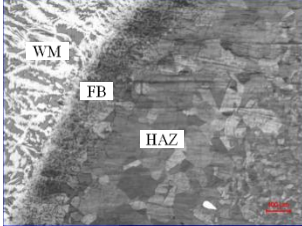
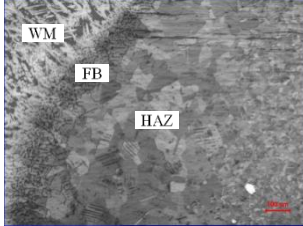
Weld backing	Welding speed (mm s^{-1})		
	1.5	2.5	3.5
Carbon steel			
Copper			
Copper with water cooled			

Table 5 Results of Dendrite and inter-dendritic spacing

Weld backing	Welding speed (m s^{-1})	Dendrite length (μm)	Inter-dendrite length (μm)
Carbon steel	5.1	152.32	40.49
	5.2	110.63	29.94
	5.3	98.47	15.47
Copper	5.1	137.46	38.52
	5.2	108.93	22.31
	5.3	83.46	13.52
Copper with water cooled	5.1	120.38	16.36
	5.2	103.91	14.90
	5.3	76.44	11.78

Table 5 Shown the results of measured values of dendrite lengths and inter-dendritic spacing for all samples, with the use of Leica image analysis program. It is revealed that the weldment was welding speed increases and high cooling rate, the dendrite size and interdendritic spacing in the weld metal reduced [9]. This dendrite size variation can be attributed to the fact that at high welding speed (low heat input)

and weld backing with high cooled. Thus, cooling rate is relatively higher due to which steep thermal gradients are established in the weld metal which in turn allow lesser time for the dendrites to grow, whereas, at low welding speed (high heat input), cooling rate is slow which provides ample time for the dendrites to grow farther into the fusion zone [10].

The illustration of microhardness profile which observed from the center of weld metal (WM), Heat affected zone (HAZ), and Fusion boundary (FB). Fig. 4 shown was reveal that HAZ of AISI 2205 was the highest microhardness than all area of the weldment, this weldment was welding with welding speed 3.5 mm s^{-1} on copper water-cooled as 295.2–307.8 HV. Lowest microhardness value at weld metal as welding with 1.5 mm s^{-1} on carbon steel as 241.1–24.4 HV.

Table 6 shown the results of tensile properties of the weldment. The highest of tensile strength as welding with welding speed 3.5 mm s^{-1} on copper water-cooled as 778.78 Mpa. Lowest tensile strength as welding with welding speed 1.5 mm s^{-1} on copper water-cooled as 725.20 Mpa. All fracture of samples was a failure at AISI 201 site. This phenomenon shows that high ultimate

tensile strength, which can attribute to smaller dendrite length and interdendritic spacing [11].

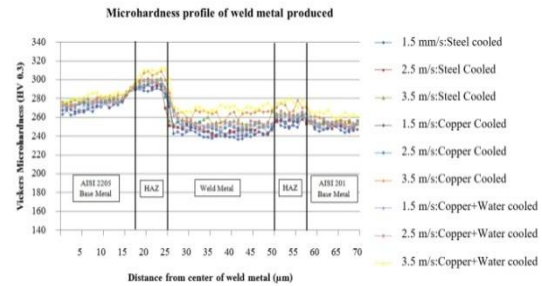


Fig. 4 Results of microhardness. Welded with welding speed at 1.5, 2.5, and 3.5 mm s^{-1} which cooled by 3 types weld backing as (Steel cooled), copper (Copper cooled), and copper with water cooled (Copper + Water cooled).

Table 6 Tensile strength test results

Weld backing	Welding speed (mm s^{-1})	Ultimate Tensile Strength (Mpa)	Elongation (%)	Failure position	Welding efficiency (%)
Carbon steel	1.5	725.20	15.45	HAZ, AISI 201 site	81.91
	2.5	726.12	15.93	HAZ, AISI 201 site	82.02
	3.5	726.96	16.14	HAZ, AISI 201 site	82.11
Copper	1.5	750.03	17.39	HAZ, AISI 201 site	84.72
	2.5	755.18	18.23	HAZ, AISI 201 site	85.30
	3.5	757.16	18.52	HAZ, AISI 201 site	85.52
Copper with water cooled	1.5	770.66	18.77	HAZ, AISI 201 site	87.05
	2.5	773.58	19.14	HAZ, AISI 201 site	87.38
	3.5	778.78	23.43	HAZ, AISI 201 site	87.96

CONCLUSION

This research has studied the effect of Gas tungsten arc welding parameters welding on the microstructure and mechanical of dissimilar weldment between Duplex Stainless Steel AISI 2205 to Austenitic Stainless Steel AISI 201. The following conclusions can be drawn.

(1) The welding speed and cooling rate increases, the length of dendrite and width of the face and root weld reduced because of the low heat input in the weld pool which influenced to the ferrite contents reduced.

(2) The maximum of microhardness and tensile strength were found that weld with welding speed 3.5 mm s^{-1} and cooling by copper plate with water cooled

REFERENCES

- [1] H. Feng, H. Jiang, D. Yan, L. Rong, Microstructure and Mechanical Properties of a CuCrZr Welding Joint After Continuous Extrusion, *J. Mater. Sci. Technol.* 31 (2015) 210–216.
- [2] N. Arivazhagan, K. Senthilkumaran, S. Narayanan, K. D. Ramkumar, S. Surendra, S. Prakash, Hot Corrosion Behavior of Friction Welded AISI 4140 and AISI 304 in K_2SO_4 -60% NaCl Mixture, *J. Mater. Sci. Technol.* 28 (2012) 895–904.
- [3] R. Badji, Phase transformation and mechanical behavior in annealed 2205 duplex stainless steel welds, *Mat. Charac.* 59 (2008) 447–453.

- [4] S.B. David, A.B. Cheryl, AL 201 HPTM (UNS S20100) alloy a high-performance, lower-nickel an alternative to 300 series alloy, Stainless Steel World 2005 Conference, Maastricht, Netherlands. 9 November 2005, 17–20.
- [5] C. Wichan, S. Loeshpahn, Effect of filler alloy on microstructure, mechanical and corrosion behavior of dissimilar weldment between AISI 201 stainless steel and low carbon steel sheets produced by a gas tungsten arc welding, *Advan. Mat. Res.* 581–582 (2012) 808–816
- [6] C. Wichan, S. Loeshpahn, Effect of welding speed on microstructures, mechanical properties and corrosion behavior of GTA-welded AISI 201 stainless steel sheets, *J. Mat. Pro. Tech.* 214 (2014) 33–37.
- [7] ASTM International, E407– 07e1: Standard Practices for Microetching Metal and Alloys, West Conshohocken, PA, USA, 2015
- [8] American Society for Metal, Selection of Wrought Duplex Stainless Steel, *Metal Handbook, Volume 6, Welding Brazing and Soldering*, 2nd ed., Ohio, ASM International, USA, 1994, pp. 471–481.
- [9] S. Kumar, A.S. Shahi, Effect of heat input on the microstructure and mechanical properties of gas tungsten arc welded AISI 304 stainless steel joints, *Mater. Des.* 32 (2011) 3617–3623.
- [10] V. Muthupandi, P.B. Srinivasan, S.K. Seshadri, S. Sundaresan, Effect of weld metal chemistry and heat input on the structure and properties of duplex stain-less steel welds, *Mat. Sci. Eng. A.* 358 (2003) 9–6.
- [11] S. Wang, Q. Ma, Y. Li, Characterization of microstructure, mechanical properties and corrosion resistance of dissimilar welded joint between 2205 duplex stainless steel and 16MnR, *Mater. Des.* 32 (2011) 831–837.